

Multiple effects of operating variables on heat transfer in three-phase slurry bubble columns

Ik Sang Shin*, Sung Mo Son*, Dae Ho Lim*, Yong Kang*,†, Heon Jung**, and Ho Tae Lee**

*School of Bio and Applied Chemical Engineering, Chungnam National University, Daejeon 305-764, Korea

**Synfuel Research Group, Korea Institute of Energy Research, Daejeon 305-343, Korea

(Received 14 August 2009 • accepted 3 November 2009)

Abstract—Characteristics of heat transfer were investigated in pressurized slurry bubble column reactors whose diameter was either 0.051, 0.076, 0.102 or 0.152 m (ID) and 1.5 m in height, respectively. Effects of gas velocity (U_g), solid contents (S_c), pressure (P), liquid viscosity (μ_l) and column diameter (D) on the heat transfer coefficient (h) between the immersed vertical heater and the column were determined. Multiple effects such as U_g and D, P and D, μ_l and D, and S_c and D on the value of heat transfer coefficient were discussed. Temperature fluctuations were also measured and analyzed by adapting chaos theory, which was used to explain the effects of operating variables on the heat transfer in the column. The heat transfer coefficient increased with increasing gas velocity, pressure or solid content in the slurry phase, but decreased with increasing liquid viscosity or column diameter. The decrease trend of h with increasing column diameter was somewhat sensitive when the gas velocity was relatively high ($U_g \geq 12$ cm/s). The effects of column diameter on the h value became almost linear when the operating pressure ($P=4-10$ kg/cm²), liquid viscosity ($\mu_l=20-38$ mPa·s) or solid content in the slurry phase ($S_c=10-20$ wt%) was relatively high and gas velocity was relatively low, within these experimental conditions. The heat transfer coefficient was well correlated in terms of dimensionless groups as well as operating variables.

Key words: Temperature Fluctuations, Heat Transfer, Slurry Bubble Column, Pressure, Viscous, Column Diameter

INTRODUCTION

Three-phase slurry bubble column reactor can be utilized for the production of synthetic liquid fuel from syngas or solid material, such as coal and biomass, effectively and economically. It has been understood that the flow behaviors of reactant gas bubbles have important factors to determine the conversion level and reaction itself, since the reactant gas phase exists as a dispersed phase in the continuous slurry medium where the solid catalyst is involved [1-3]. Therefore, several investigations have been conducted on the hydrodynamics, bubble properties and heat and mass transfer in three-phase slurry bubble columns and reactors [4-10]. For the development of GTL (gas-to-liquid) and CTL (coal-to-liquid) processes and reactors, the reactor volume and reaction time should be properly adjusted to meet the economic conversion as well as production level and rate of the products.

There have been several investigations on the slurry bubble column reactors, however, most of them were conducted in laboratory scale reactors. For the commercial design or scale-up of the pressurized slurry bubble column reactor, the information on the design and scale-up of the reactor in commercial scale has been essential. Especially, for the reactor or process performing a heterogeneous reaction including multiphase contacting, the information for the design and scale-up technology has been limited for lack of limited data and technology [11,12]. In addition, the understanding of the heat transfer characteristics with increasing column diameter is essen-

tial, because the similarity of heat transfer rate or reaction temperature should be adjusted properly with increasing column diameter. It has been generally understood that, in dynamic flow systems such as slurry bubble column reactors, the thermal stability and similarity have to be controlled and adjusted to provide the heterogeneous reactants with plausible conditions for effective contacting and reaction.

However, there has been little attention to the design and scale up of such reactors and contactors in view of similarity and stability, with the variation of column diameter. Thus, in the present study, multiple effects of operating variables on the heat transfer characteristics with variation of column diameter were examined to predict the information in designing the multiphase slurry bubble column reactors.

EXPERIMENTS

Experiments were carried out in stainless-steel columns whose inside diameter was either 0.058, 0.076, 0.102 or 0.152 m and 1.5 m in height, as can be seen in Fig. 1 [9,13]. The gas distributor was installed between the main column section and a 0.2 m high stainless-steel distributor box. Oil-free compressed air was fed to the column through a pressure regulator, filter and a calibrated air flowmeter. It was admitted to the column through 3.0 mm ID perforated pipe drilled horizontally in the grid. The superficial velocity of gas phase ranged from 0.02-0.16 m/s, the pressure ranged from 0.1-1.0 MPa and the viscosity of liquid phase ranged from 1.0-38.0 mPa·s, respectively. The physical properties of liquid phase were listed in Table 1. Glass bead whose diameter was in the range of 40-70 μ m was used to comprise the slurry phase. The concentra-

*To whom correspondence should be addressed.

E-mail: kangyong@cnu.ac.kr

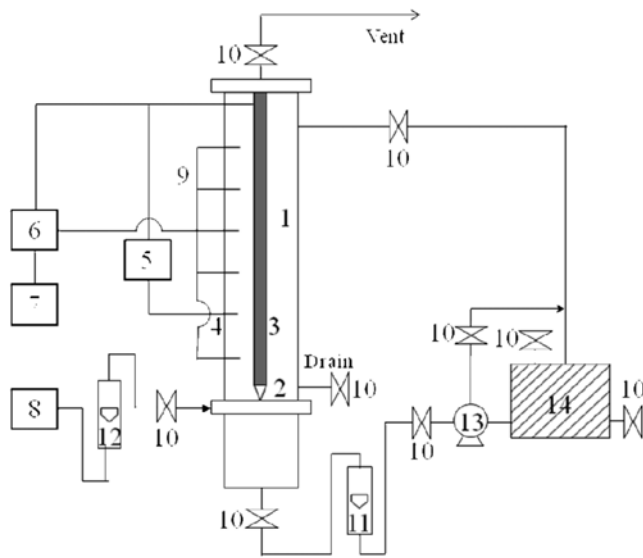


Fig. 1. Schematic diagram of experimental apparatus.

1. Main column	8. Compressor
2. Gas distributor	9. Pressure tap
3. Heater	10. Valve
4. Thermocouple	11. Liquid flowmeter
5. Digital indicator	12. Gas flowmeter
6. A/D converter	13. Slurry pump
7. Computer	14. Slurry reservoir

tion of solid in the slurry phase was in the range of 0-20 wt%.

The ΔT -fluctuations between the heater surface and the column proper were measured by iron-constantan thermocouples (J-type). As a heating source, a cone-shaped heater with an outside diameter of 0.03 m and a length of 1.0 m was placed coaxially on the distributor plate at the center of the column. Four thermocouple probes were installed at the center of the annulus between the heater and the column wall, at 0.2 m above the distributor with the axial interval of 0.2 m. Five thermocouple probes were also attached at the surface of the heater to measure the heater surface temperatures. These probes were connected to a temperature indicating system, data acquisition system (Data Precision Model, DT 3001) and a personal computer to record simultaneously and continuously all points temperatures. The voltage-time signals, corresponding to the temperature-time signals, were sampled at a rate of 0.002 s and stored in the data acquisition system. The total acquisition time was 10 s having 5000 data points. This combination of sampling rate and time can detect the full spectrum of temperature fluctuation signals in a multiphase flow system [13-16].

When a steady state was reached, the temperatures were mea-

sured repeatedly. The heat transfer coefficients were determined by Eq. (1),

$$h = \frac{Q}{A(T_h - T_c)} \quad (1)$$

From the knowledge of heat supply and mean temperature difference between the heater surface and the column proper. The heat supply, Q , was obtained from the DC power supply, and it was verified from the energy balance in the riser. Individual phase holdups were determined by means of static pressure drop method [17-20].

To estimate the correlation dimension of the time-series of temperature fluctuations, $X(t)$, their trajectories, reconstructed by resorting to time embedding have been used. From the trajectories of the vector time series, the correlation integral (the space correlation function) of the process, $C(r)$, which is defined as Eq. (2), was calculated [15,16,21].

$$C(r) = \lim_{m \rightarrow \infty} \frac{1}{m^2} [\text{number of pairs } (i, j) \text{ whose distance } |Z_i(t) - Z_j(t)| < r] \quad (2)$$

Formally,

$$C(r) = \lim_{m \rightarrow \infty} \frac{1}{m^2} \sum_{i=1}^m \sum_{j=1}^m H[r - |Z_i(t) - Z_j(t)|], \quad i \neq j, \quad (3)$$

where m is the number of data points, and H is the Heaviside function, which can be expressed as

$$H[r - |Z_i(t) - Z_j(t)|] = \begin{cases} 1 & \text{if } r > |Z_i(t) - Z_j(t)|, \\ 0 & \text{otherwise} \end{cases} \quad (4)$$

The correlation integral, $C(r)$, has been found to be a power function of r for small r 's:

$$C(r) = kr^{D_c} \quad (5)$$

Since the slope of the plot of $\ln C(r)$ vs. $\ln r$ is an estimate of D_c , for the given embedded space dimension, P , the correlation dimension of temperature fluctuations was determined by means of Eqs. (2)-(5).

RESULTS AND DISCUSSION

A typical example of normalized temperature difference fluctuations between the heater surface and the column proper (ΔT) can be seen Fig. 2. The mean value of ΔT in a given operating condition was obtained from these time series of signals to calculate the value of heat transfer coefficient (h).

Effects of U_G and D on the heat transfer coefficient can be seen

Table 1. Physical and rheological properties of liquid phase

	Dynamic viscosity (mPa·s)	Surface tension (mN/m)	Density (kg/m ³)	K (Pa·s ⁿ)	n	Diffusivity (cm ² /s)	Kinematic viscosity (m ² /s)
Water	0.961	72.9	1000	0.001	1	2.22×10^{-5}	9.61×10^{-7}
CMC 0.1 wt%	11	73.2	1001	21.69×10^{-3}	0.882	0.48×10^{-5}	1.10×10^{-5}
CMC 0.2 wt%	24	73.3	1002	43.82×10^{-3}	0.847	0.26×10^{-5}	2.40×10^{-5}
CMC 0.3 wt%	38	73.6	1003	71.69×10^{-3}	0.825	0.19×10^{-5}	3.79×10^{-5}

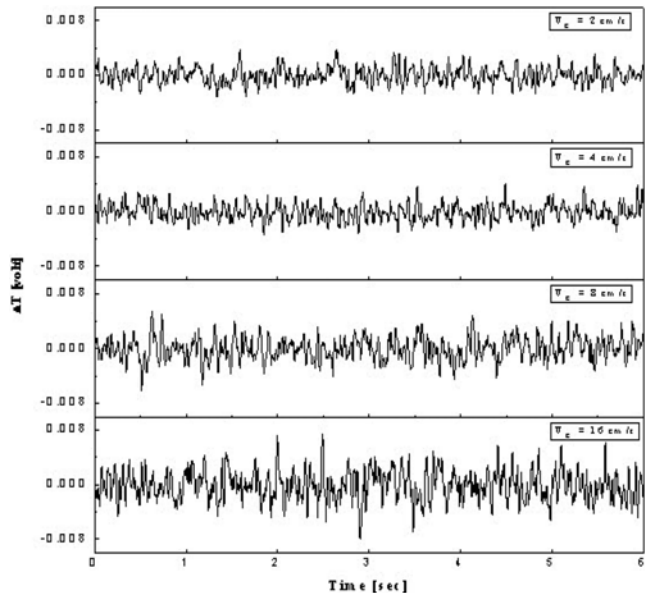


Fig. 2. Typical examples of normalized temperature difference fluctuations in three-phase slurry bubble columns ($S_c=10$ wt%, $P=8$ kg/cm 2 , $\mu_L=24$ mPa·s).

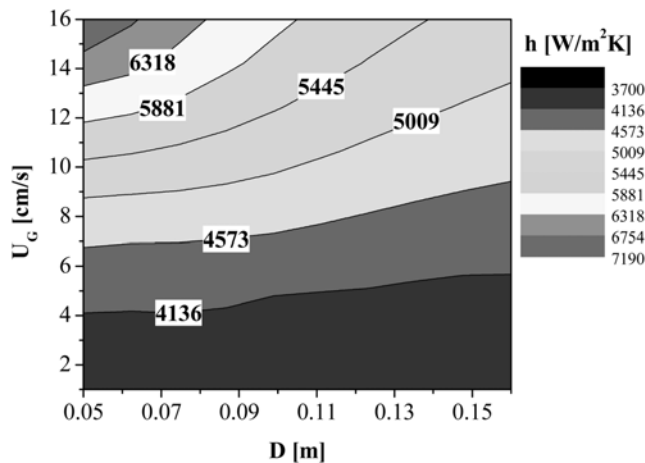


Fig. 3. Contour map of heat transfer coefficient with variations of U_G & D in three-phase slurry bubble columns ($S_c=20$ wt%, $P=8$ kg/cm 2 , $\mu_L=24$ mPa·s).

in Fig. 3. As expected, the value of h increases with increasing U_G , but the increase trend of h with increasing U_G becomes insensitive with an increase in column diameter. In addition, the value of h in a given U_G decreases gradually with increasing column diameter (D). Note that in this figure the decreasing trend of h with increasing D becomes considerable with increasing U_G . These phenomena can be explained by means of bubbling behavior in the column. That is the bubble size and frequency and thus its holdup increase with increasing U_G , but the bubble holdup decreases with increasing column diameter. In addition, the decreasing trend of bubble holdup with increasing column diameter becomes significant with increasing U_G . Therefore, it would be reasonable to state that the value of h increases with increasing bubble holdup in slurry bubble column reactors. It has been understood that the turbulence inten-

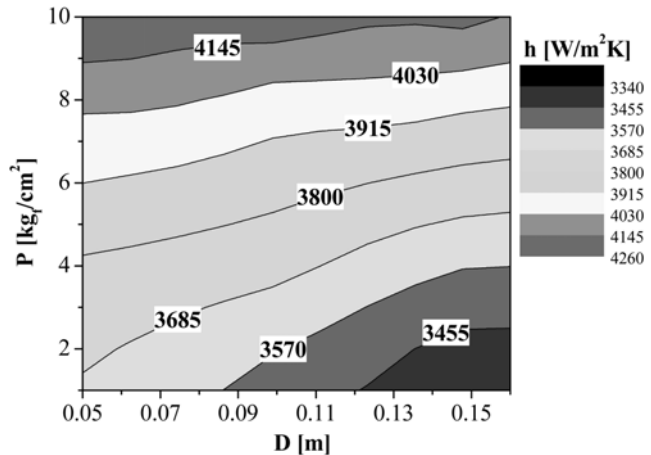


Fig. 4. Contour map of heat transfer coefficient with variations of P & D in three-phase slurry bubble columns ($S_c=20$ wt%, $U_G=2$ cm/s, $\mu_L=24$ mPa·s).

sity in the reactor increases with increasing bubble holdup, since the bubbles exist as a dispersed phase in the continuous slurry medium [7-10]. These imply that the effects of column diameter on the heat transfer coefficient would be considerable when the gas velocity is in the relatively high range. Specifically, when the gas velocity is higher than 12 cm/s, the decreasing trend of the heat transfer coefficient with increasing column diameter becomes somewhat considerable within experimental conditions.

Effects of pressure and column diameter on the heat transfer coefficient can be seen in Fig. 4, where the value of h increases with pressure. While the decreasing trend of h with increasing D is somewhat sensitive when the operating pressure is under 3 kg/cm 2 , the decreasing trend of h with increasing column diameter is reduced and the ratio becomes almost linear, when the pressure is over 4 kg/cm 2 . This means that the effects of column diameter on the heat transfer coefficient become almost linear when the operating pressure is relatively high ($P=4-10$ kg/cm 2) and the gas velocity is relatively low ($U_G=6$ cm/s) (Figs. 3 and 4).

Since the heat transfer phenomenon is closely related to the temperature fluctuations in the columns, the temperature fluctuations were measured and analyzed by adapting chaos theory. More specifically, the correlation dimension of temperature fluctuations was determined by embedding the trajectories in the phase-space dimension, since the attractor dimension essentially converges with increasing embedding dimension [15,16,21]. From the repeated calculation with different random samples, the attractor dimension converged when the estimated values were less than 3.5% within experimental conditions. Five of six dimensions of phase space were required in the embedding space in order to capture the topological features of the attractor. Effects of gas velocity and column diameter on the correlation dimension (D_c) of temperature fluctuations can be seen in Fig. 5. In this figure, the value of D_c increases with increasing gas velocity, but decreases with increasing column diameter. Since the correlation dimension is a measure of the spatial homogeneity in the state space [13,15,21], this implies that the heat transfer field becomes non-homogeneous and more chaotic with increasing U_G , however, the field becomes more homogeneous with increasing column diameter. In other words, the temperature fluctuation be-

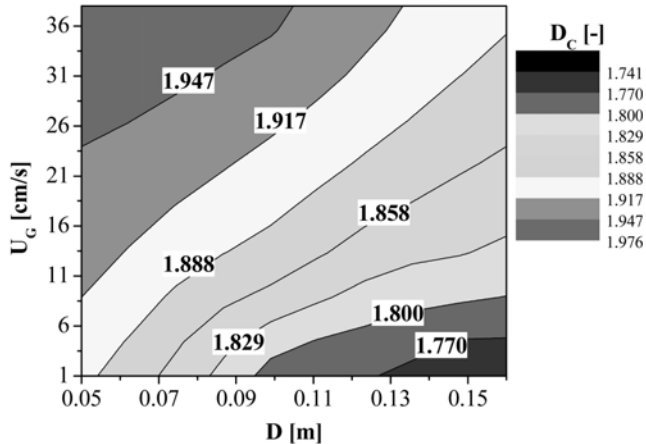


Fig. 5. Contour map of correlation dimension of temperature fluctuations with variations of U_g & D in three-phase slurry bubble columns ($S_c=20$ wt%, $P=8$ kg/cm 2 , $\mu_L=24$ mPa·s).

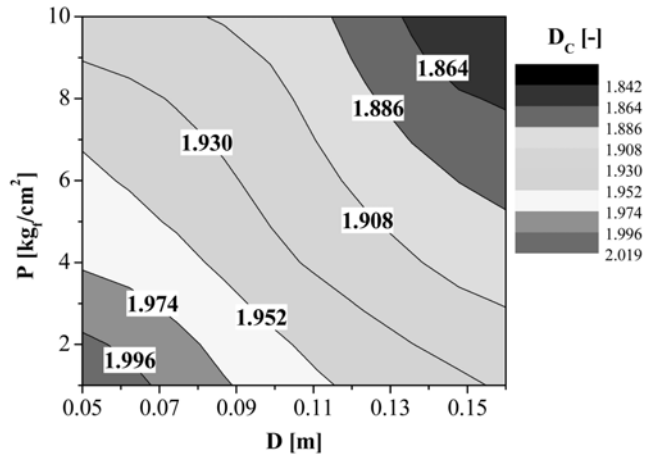


Fig. 6. Contour map of correlation dimension of temperature fluctuations with variations of P & D in three-phase slurry bubble columns ($S_c=20$ wt%, $U_g=2$ cm/s, $\mu_L=24$ mPa·s).

comes vigorous owing to the increase of holdup of discrete bubble phase, because the turbulence intensity and scale would increase with increasing gas holdup, which is a result of the increase of gas velocity. It has been understood that the heat transfer coefficient increases with increasing turbulence intensity in multiphase fluidized beds [16-20]. This can be the reason why the h value increases with increasing U_g (Fig. 3).

Effects of pressure and column diameter on the correlation dimension of temperature fluctuations can be seen in Fig. 6. In the figure, the value of the correlation dimension of temperature fluctuations decreases with increasing pressure or column diameter. This means that the stability of the heat transfer system increases with increasing pressure, since the bubble size decreases and its frequency increases with increasing pressure. This condition could let the heat transfer coefficient increase, because the more frequent bubble contacting at the heater surface as well as column proper could lead to the heat to be transferred more conveniently. That is the more regular motion of relatively small bubbles in the column could promote the effective turbulence for heat transfer in this column, with in-

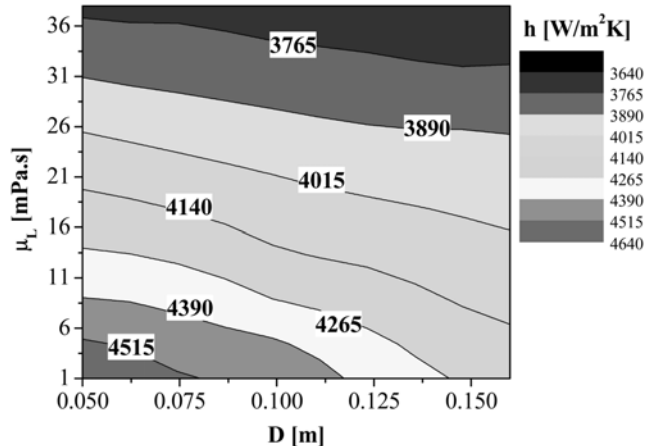


Fig. 7. Contour map of heat transfer coefficient with variations of μ_L & D in three-phase slurry bubble columns ($S_c=10$ wt%, $U_g=2$ cm/s, $P=4$ kg/cm 2).

creasing the pressure of the system. It has been understood that the bubble holdup increases but its size decreases, with increasing pressure. It has been understood that the smaller the bubble size the more periodic and regular the flow behavior of bubbles in the column. This can be the reason why the value of h could increase with increasing the pressure of the system. In Figs. 5 and 6, the value of D_c decreases with increasing column diameter. This implies that the system becomes stable with increasing column diameter, which can be due to the decrease of bubble holdup compensating for the increase in continuous slurry phase, with increasing column diameter. Note that the increase of column diameter could lead to the increase of stability of the system; however, it also leads to the decrease of turbulence intensity owing to the decrease of bubble holdup. Thus the value of h decreases although the value of D_c decreases, with increasing column diameter (Figs. 4 and 6).

Effects of liquid viscosity (μ_L) and column diameter on the heat transfer coefficient can be seen in Fig. 7. Note in this figure that the h value decreases with increasing liquid viscosity (μ_L). In addition, the decreasing trend of h with increasing D becomes almost linear when the liquid viscosity is in the range of 20-38 mPa·s, but the decreasing trend of h with D is relatively sensitive when the liquid viscosity is in the range of 1.0-13 mPa·s. It can be stated from this figure that the effects of column diameter on the h value become almost linear when the liquid viscosity is relatively high ($\mu_L=20-38$ mPa·s) and gas velocity is relatively low ($U_g \leq 4$ cm/s).

Effects of solid content in the slurry phase (S_c) and column diameter on the heat transfer coefficient can be seen in Fig. 8. In this figure, the value of h increases with solid content in the slurry phase. In Fig. 8, the decreasing trend of h with increasing D becomes almost linear when the S_c is in the range of 10-20 wt%, but the decreasing trend of h with D is relatively sensitive when the S_c is in the range of 2-8 wt%. Thus, it can be stated that the effect of column diameter on the heat transfer coefficient becomes almost linear when the solid content in the slurry phase is relatively high ($S_c=10-20$ wt%) and gas velocity is relatively low.

Effects of slurry viscosity and column diameter on the correlation dimension of temperature fluctuations can be seen in Fig. 9. Note in this figure that the value of D_c increases with increasing liquid viscos-

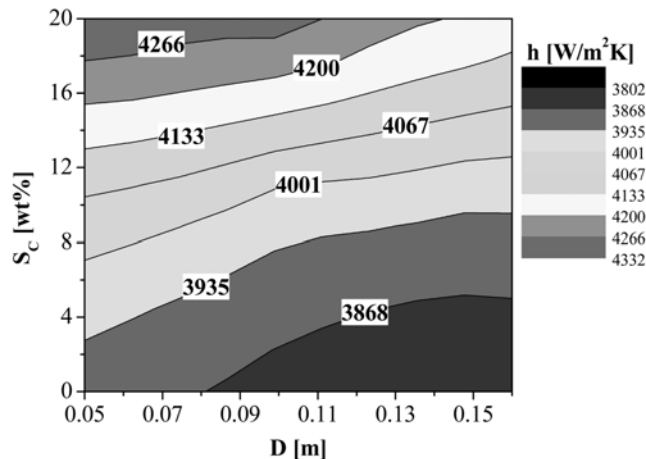


Fig. 8. Contour map of heat transfer coefficient with variations of S_c & D in three-phase slurry bubble columns ($\mu_L=24 \text{ mPa}\cdot\text{s}$, $U_G=4 \text{ cm/s}$, $P=8 \text{ kg/cm}^2$).

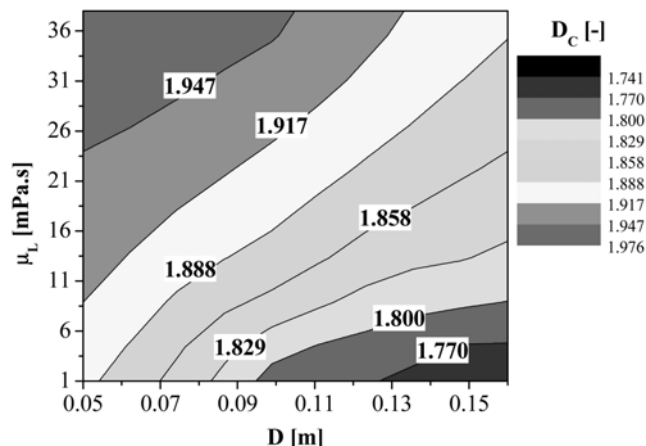


Fig. 9. Contour map of correlation dimension of temperature fluctuations with variations of μ_L & D in three-phase slurry bubble columns ($S_c=10 \text{ wt\%}$, $U_G=2 \text{ cm/s}$, $P=4 \text{ kg/cm}^2$).

ity and decreases with increasing column diameter. This means that the stability of the heat transfer field decreases with increasing liquid viscosity. This can be because the bubble size increases with increasing liquid viscosity thus the distribution of bubble size becomes wider with increasing liquid viscosity. In other words, the wider distribution of bubble size could lead to the more irregular flow motion of bubbles in the vicinity of heater surface as well as in the column proper. In addition, the increase of liquid viscosity could lead to the bubble motion to be restricted owing to the increase of viscous force acting on the flowing bubbles, which consequently results in the decrease of free regular flow motion in the column. Therefore, the h value decreases with increasing liquid viscosity.

Effects of solid content in the slurry phase (S_c) and column diameter on the correlation dimension of temperature fluctuations can be seen in Fig. 10. In this figure, the value of D_c decreases gradually with increasing solid content in the slurry phase or column diameter. This means that the heat transfer field becomes more stable with increasing S_c . This can be due to the fact that the heat conductivity of solid particles in the slurry phase is higher than that of liquid

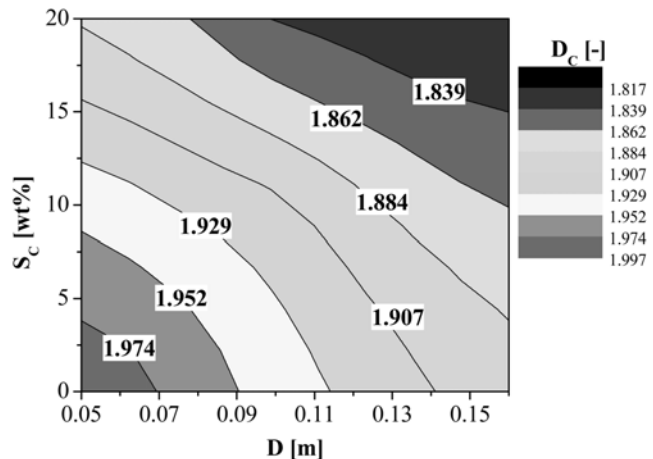


Fig. 10. Contour map of correlation dimension of temperature fluctuations with variations of S_c & D in three-phase slurry bubble columns ($\mu_L=24 \text{ mPa}\cdot\text{s}$, $U_G=4 \text{ cm/s}$, $P=8 \text{ kg/cm}^2$).

phase, thus, the heat transfer from the heater surface to the column proper would be more convenient with increasing S_c . This could be the reason why the h value increases with increasing S_c (Fig. 8).

The value of heat transfer coefficient was well correlated in terms of dimensionless groups as Eq. (6), with a correlation coefficient of 0.92 within experimental conditions of this study.

$$Nu = \frac{hd_p(1-\varepsilon_s)}{k_L \varepsilon_s} = 1.56 \left(\frac{C_{PL} \mu_L}{k_L} \right)^{0.26} \left(\frac{d_p \rho_L U_G}{\mu_L \varepsilon_s} \right)^{0.31} \left(\frac{d_p}{D} \right)^{0.07} \left(\frac{P}{P_0} \right)^{0.12} \quad (6)$$

CONCLUSION

The heat transfer coefficient increased with increasing gas velocity, pressure or solid content in the slurry phase, but decreased with increasing liquid viscosity or column diameter. The increasing trend of h with increasing U_G became insensitive with increasing column diameter, however, the decreasing trend of h with increasing column diameter was somewhat sensitive when the gas velocity was relatively high ($U_G \geq 12 \text{ cm/s}$). The effect of column diameter on the h value became almost linear when the operating pressure ($P=4-10 \text{ kg/cm}^2$), liquid viscosity ($\mu_L=20-38 \text{ mPa}\cdot\text{s}$) or solid content in the slurry phase ($S_c=10-20 \text{ wt\%}$) was relatively high and gas velocity was relatively low, within these experimental conditions. The correlation dimension of temperature fluctuations could be employed to analyze the heat transfer phenomena in the pressurized slurry bubble columns.

ACKNOWLEDGMENT

Financial support from Korea Energy Research Institute (A7-2802) is greatly appreciated.

NOMENCLATURE

A : surface area of heater [m^2]

C_{PL} : heat capacity of liquid phase [$\text{kcal/kg}\cdot\text{K}$]

$C(r)$: correlation integral

D	: column diameter [m]
D_c	: correlation dimension [-]
d_p	: particle diameter [m]
H	: Heaviside function defined as in Eq. (4)
h	: heat transfer coefficient [W/m ² ·K]
k_L	: conductivity of liquid phase [W/m·K]
m	: number of data points
Nu	: Nusselt number [-]
P	: pressure [kg/cm ²]
P_0	: standard pressure [kg/cm ²]
r	: radius of hyper sphere
Q	: heat flow [W]
S_c	: solid content [wt%]
t	: time [s]
T_C	: column temperature [K]
T_h	: heater surface temperature [K]
ΔT	: mean temperature difference [K]
U_G	: superficial gas velocity [cm/s]
X(t)	: time series of pressure fluctuations [MPa]
Z_i	: the vector time series

Greek Letter

ε_s	: solid holdup [-]
μ_L	: liquid viscosity [mPa·s]
ρ_{SL}	: slurry density [kg/m ³]

REFERENCES

1. L. S. Fan, *Gas-liquid-solid fluidization engineering*, Butterworth, Boston (1989).
2. W.-D. Deckwer, *Bubble column reactor*, John Wiley and Sons, New York (1992).
3. S. D. Kim and Y. Kang, *Chem. Eng. Sci.*, **52**, 3639 (1997).
4. J. Drahos, F. Bradka and M. Puncochar, *Chem. Eng. Sci.*, **47**, 4069 (1992).
5. L. T. Fan, Y. Kang, D. Neogi and M. Yashima, *AIChE J.*, **39**, 513 (1993).
6. Y. J. Cho, S. J. Kim, S. H. Nam, Y. Kang and S. D. Kim, *Chem. Eng. Sci.*, **56**, 6107 (2001).
7. S. D. Kim, Y. Kang and H. K. Kwon, *AIChE J.*, **32**, 1397 (1986).
8. R. Krishna, J. W. A. de Swart, J. Ellenbeger, G. V. Martina and C. Maretto, *AIChE J.*, **43**, 311 (1997).
9. I. S. Shin, S. M. Son, U. Y. Kim, Y. Kang, S. D. Kim and H. Jung, *Korean J. Chem. Eng.*, **26**, 587 (2009).
10. R. Krishna and S. T. Sie, *Fuel Processing Technol.*, **64**, 73 (2000).
11. R. Krishna, R. Lemoine, L. Sehabiaque, R. Oukaci and B. I. Morsi, *Chem. Eng. J.*, **128**, 69 (2007).
12. C. Maretto and R. Krishna, *Catal. Today*, **52**, 279 (1999).
13. Y. Kang, Y. J. Cho, K. J. Woo, K. I. Kim and S. D. Kim, *Chem. Eng. Sci.*, **55**, 411 (2000).
14. S. H. Kang, S. M. Son, Y. Kang, J. W. Bae and K. W. Jun, *Korean J. Chem. Eng.*, **25**, 897 (2008).
15. Y. Kang, Y. J. Cho, K. J. Woo and S. D. Kim, *Chem. Eng. Sci.*, **54**, 4887 (1999).
16. J. S. Kim, K. J. Woo, Y. Kang, C. H. Nam and S. D. Kim, *J. Chem. Eng. Japan*, **34**, 185 (2001).
17. S. M. Son, I. S. Shin, S. H. Kang, Y. Kang and S. D. Kim, *Korean J. Chem. Eng.*, **24**, 866 (2007).
18. U. Y. Kim, S. M. Son, S. H. Kang, Y. Kang and S. D. Kim, *Korean J. Chem. Eng.*, **24**, 892 (2007).
19. S. M. Son, K. I. Lee, S. H. Kang, Y. Kang and S. D. Kim, *AIChE J.*, **53**, 3011 (2007).
20. K. S. Shin, K. J. Woo, Y. Kang, C. H. Nam and S. D. Kim, *J. Chem. Eng. Japan*, **34**, 185 (2001).
21. P. Grassberger and I. Procaccia, *Physica. D.*, **9**, 189 (1983).